



## A study on the nickel(II)-famotidine complexes

Małgorzata Barańska<sup>a</sup>, Elżbieta Gumienna-Kontecka<sup>b</sup>, Henryk Kozłowski<sup>b</sup>,  
Leonard M. Proniewicz<sup>a,c,\*</sup>

<sup>a</sup>Faculty of Chemistry, Jagiellonian University, 3 Ingardena Str., 30-060 Cracow, Poland

<sup>b</sup>Faculty of Chemistry, University of Wrocław, 14 F. Joliot-Curie Str., 50-383 Wrocław, Poland

<sup>c</sup>Regional Laboratory of Physicochemical Analysis and Structural Research, Jagiellonian University, 3 Ingardena Str., 30-060 Cracow, Poland

Received 20 December 2001; received in revised form 21 May 2002; accepted 24 May 2002

### Abstract

Potentiometric studies have shown that Ni(II) forms three pH-dependent complexes with famotidine (L), namely:  $[\text{NiHL}]^{3+}$ ,  $[\text{NiL}]^{2+}$  and  $[\text{NiH}_2\text{L}]$ . Two of them have been isolated from solution with a Ni/famotidine ratio of 1:1. At pH 6.0, a paramagnetic complex  $[\text{NiL}]^{2+}$  with octahedral geometry is formed in which, most likely thiazole N(9) and guanidine N(3) nitrogens are involved in the metal binding. Additionally, two water molecules and two perchlorate anions,  $\text{ClO}_4^-$ , fulfil the coordination sphere. The second complex,  $[\text{NiH}_2\text{L}]$ , that precipitates at pH 8 is diamagnetic and takes square-planar geometry in which four nitrogen donors: N(3), N(9), N(16) and N(20) coordinate to Ni(II). Potentiometric studies, mass spectrometry, FT-IR and Raman spectroscopy are employed to determine and discuss the structure of both complexes. Additionally,  $^1\text{H}$ ,  $^{13}\text{C}$  and  $^{15}\text{N}$  NMR spectroscopy is used to confirm the binding site in a square-planar complex. The assignment of vibrational bands are made using ab initio HF/CEP-31G method.

© 2002 Elsevier Science Inc. All rights reserved.

**Keywords:** Famotidine; Ni(II) complexes; Antulcer drugs

### 1. Introduction

Famotidine (**fam**), 3-[2-(diaminomethyleneamino)-thiazol-4-yl]-methylsulfanyl -  $\text{N}^2$  - sulfamoylpropionamide, is a histamine  $\text{H}_2$ -receptor antagonist that is more effective than the earlier used cimetidine [1,2]. Both these drugs have been used for treatment of peptic ulcers and Zollinger–Ellison syndrome. Cu(II) ions were shown to increase dramatically the cimetidine binding to imidazole receptors located in rat brain [1] and as Cu(II)-cimetidine complex exhibit unusually high superoxide dismutase-like activity. The chemical formula of **fam** together with the atomic numbering for convenience is shown in Fig. 1. The presence of amino, amido and thioether groups in its structure causes this drug to possess chelating properties and it may interact very effectively with the essential metal ions present in blood plasma and different tissues.

Earlier studies on the binding ability of **fam** have shown that this drug is able to coordinate cupric ion even at pH

below 2 to form a stable complex [3,4]. However, this has no serious impact on the distribution and availability of Cu(II) ions in living organisms. X-Ray data obtained for a single crystal of Cu(II)-**fam** complex showed that Cu(II) coordinated to **fam** molecule through guanidine N(3) and thiazole N(9) nitrogen atoms, thioether sulfur S(11) from aliphatic chain and terminal amidine nitrogen N(15) atom [4]. It has to be emphasized that this has been the only available report, so far, on the solid state metal ion complex of famotidine.

Additional  $^1\text{H}$  NMR, spectrophotometric and potentiometric studies showed that platinum(II) and palladium(II) ions effectively bind famotidine in aqueous solutions [5,6]. However, no detailed discussion on structures of these complexes was presented.

Potentiometric, polarographic and UV–Vis results were also obtained for the Ni(II)-**fam** system [1]. It was shown that Ni(II) formed two complexes:  $[\text{NiL}]^{2+}$  and  $[\text{NiH}_2\text{L}]$ , the former being octahedral, the latter having planar geometry. According to this work [1], coordination of Ni(II) began above pH 5 and the monodentate nitrogen coordination of the thiazole nitrogen was suggested for

\*Corresponding author. Fax: +48-12-634-0515.

E-mail address: [proniewi@chemia.uj.edu.pl](mailto:proniewi@chemia.uj.edu.pl) (L.M. Proniewicz).

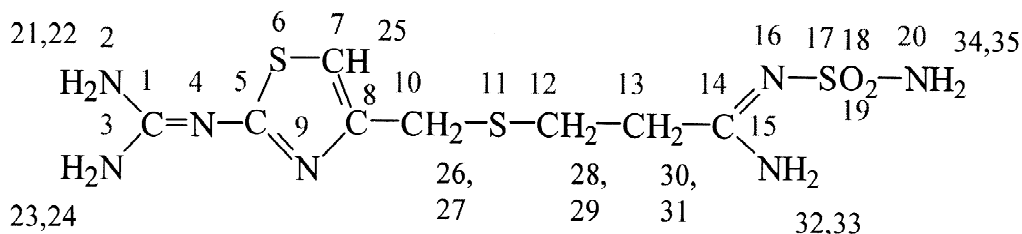


Fig. 1. Atom numbering of a molecule of famotidine.

$[\text{NiL}]^{2+}$  species. Increase of pH above 7.5 triggered the changes from the octahedral geometry of  $[\text{NiL}]^{2+}$  into square-planar. Simultaneously, two protons were released to form  $[\text{NiH}_2\text{L}]$ . The involvement of other **fam** nitrogens in complex formation seemed to be obvious but no detailed analysis of the binding sites for either of the two Ni(II) complexes was presented [1].

In this work, a continuation of our earlier interest in famotidine, its model compounds and their structures with metal ions [7,8], we present the spectroscopic characterization of two solid state nickel(II)-**fam** complexes. Potentiometry, Raman and FT-IR were used to characterize complexes with octahedral (crystallized from solution at pH 6) and square-planar geometry (precipitated at pH 8). Additionally,  $^1\text{H}$ ,  $^{13}\text{C}$  and  $^{15}\text{N}$  NMR spectroscopy was used to study the diamagnetic Ni(II)-**fam** yellowish complex. A computational analysis at the Hartree–Fock level with the CEP-31G basis set was carried out in order to calculate the geometrical structure and vibrational spectra. Since the octahedral Ni(II) complex formed has some common features with previously described octahedral Cu(II) complex thus, we primarily focus our attention on a square-planar complex that is somehow unique in such coordination.

## 2. Experimental

Famotidine of the highest grade was a gift from Polfa Pharmaceutical Co. (Starogard Gdański, Poland) and used without further purification.

### 2.1. Compound preparation

Nickel(II) complexes of **fam** were synthesized by adding dropwise Ni(II)( $\text{ClO}_4$ )<sub>2</sub> or Ni(II)( $\text{NO}_3$ )<sub>2</sub> aqueous solution to vigorously stirred hot (80 °C) aqueous solution of **fam** till the ratio of metal to ligand reached 1:1. The pH of solution was controlled and adjusted with 0.01 M NaOH, if necessary. Blue Ni(II) complex precipitated at pH 6, whereas at pH 8 Ni(II)-**fam** precipitates as yellowish-orange powder. After cooling to room temperature, complexes thus obtained were filtered out, washed twice with distilled water and stored in a desiccator over  $\text{P}_2\text{O}_5$ . As expected from the above synthesis procedure, the Ni(II) to **fam** ratio was confirmed to be 1:1 by elemental analysis

and mass spectrometry (Calc.  $\text{NiH}_2\text{L}$  yellowish-orange  $\text{C}_8\text{H}_{13}\text{N}_7\text{S}_3\text{O}_2\text{Ni}$ : C, 24.4; H, 3.3; N, 24.9. Found: C, 24.4; H, 3.2; N, 24.5).

### 2.2. Spectroscopic measurements

Raman measurements were done at room temperature by exposing pure complexes to the 514.5 nm laser line from a Spectra-Physics model 2025. Laser power at the sample was maintained at 20 mW. Raman spectra were obtained with a Spex model 1403 Czerny–Turner double monochromator equipped with a DM1B spectroscopy lab coordinator and a Hamamatsu R928 photomultiplier. Spectral band-pass was  $4\text{ cm}^{-1}$ . As many as eight spectra were accumulated for each complex. The accuracy of the frequency reading was  $\pm 1\text{ cm}^{-1}$ .

A standard procedure was used to prepare samples for IR measurements, i.e. metal complexes were dispersed in spectroscopic grade KBr (3 mg/200 mg) to form discs. Spectra were measured on a Bruker spectrometer model IFS 48 with a resolution of  $4\text{ cm}^{-1}$ . In total, 128 scans were collected for all samples. The accuracy of the frequency readings for all IR spectra was  $\pm 1\text{ cm}^{-1}$ .

All NMR measurements were done on a Bruker model AMX 500 MHz spectrometer. **Fam** and its nickel complex were dissolved in  $\text{DMSO-}d_6$  (concentration of the samples about  $10^{-3}\text{ M}$ ), transferred to a capillary and measured.  $^1\text{H}$  NMR spectra were measured with  $\text{Me}_4\text{Si}$  as an internal standard,  $^{13}\text{C}$  NMR spectra were recorded with a resonance frequency of 125.77 MHz. Pick from solvent (39.5 ppm) was used as the calibration of the scale of chemical shifts. About 4000 scans were obtained for sample spectra.  $^{15}\text{N}$  NMR spectra of **fam** and its square-planar complex with proton decoupling were recorded in a 10-mm sample tube. Nitromethane resonance frequency at 380.23 ppm was used as an external standard. All measurements were done at 300 K.

### 2.3. Potentiometric studies

Titrations involved an ionic background of 0.1 M  $\text{KNO}_3$ , ligand concentration of 2 mM and metal-to-ligand ratios of 1:3 and 1:4. Initial solutions of 2 ml were titrated with sodium hydroxide delivered by a 0.25-ml micrometer syringe previously calibrated by weight titrations and titrations of standard materials. The pH-metric titrations

were carried out at 25 °C, over the 2–8.0 pH range due to complex precipitation in more basic solutions, using a MOLSPIN automatic titration system with a Russell CMAW 711 micro-combined electrode calibrated daily in hydrogen-ion concentration using HNO<sub>3</sub> [9]. The SUPER-QUAD computer program was used for calculations of stability constants ( $\beta_{pqr} = [M_p H_r L_q] / [M]^p [H]^r [L]^q$ ) [10]. Standard deviations quoted refer to random errors only. They are, however, a good indication of the importance of a particular species in the equilibrium.

#### 2.4. Quantum-chemical calculations

Calculations were carried out at the ab initio Hartree–Fock level with basis set CEP-31G implemented in GAUSSIAN '98 program. Computations of square-planar nickel complex were done at the Academic Computer Center 'Cyfronet' in Cracow. First the geometry of the complex was optimized. Then the frequencies of all vibrational modes were analytically calculated assuming C<sub>1</sub> group symmetry [11]. No imaginary vibrational frequencies were obtained for optimized geometry of the complex. Normal mode analysis was done visually with the ANIMOL and MOLDEN programs. Calculated vibrational frequencies were multiplied by an empirical factor of 0.89 to account for the usual overestimation of vibrational frequencies due to vibrational anharmonicity and neglecting electron correlation [12,13]. Thus calculated vibrational modes were assigned to match against experimental data and, additionally, checked to be in agreement with characteristic group frequencies [14–16].

### 3. Results and discussion

#### 3.1. Potentiometric results

Potentiometric studies have shown that **fam** forms three complexes with Ni(II) within the pH range of 2.0–8.0, namely: [NiHL]<sup>3+</sup>, [NiL]<sup>2+</sup> and [NiH<sub>2</sub>L]. The first two complexes are octahedral and they predominate at pH 5.0–7.5 while the latter species is a square-planar complex that dominates above pH 8.0 (Fig. 2). The data obtained here differs distinctly from those reported earlier [1], i.e. we propose formation of two instead of one species in the pH range of 5.0–7.5. The main reason derives from the fact that in the earlier studies, only one protonation constant was assumed.

Solution studies and X-ray structure of the Cu(II) **fam** complex, [CuL][ClO<sub>4</sub>]<sub>2</sub>, have shown that the guanidine moiety may act as an anchor and the thiazole nitrogen N(9) with protonation constant around 6.7 may close the chelate ring to form the [ML]<sup>2+</sup> species. This could be a case for a blue Ni(II) **fam** complex. The low stability of the [NiHL]<sup>3+</sup> complex could be derived from the minor, if any, impact of guanidine nitrogens on the complex forma-

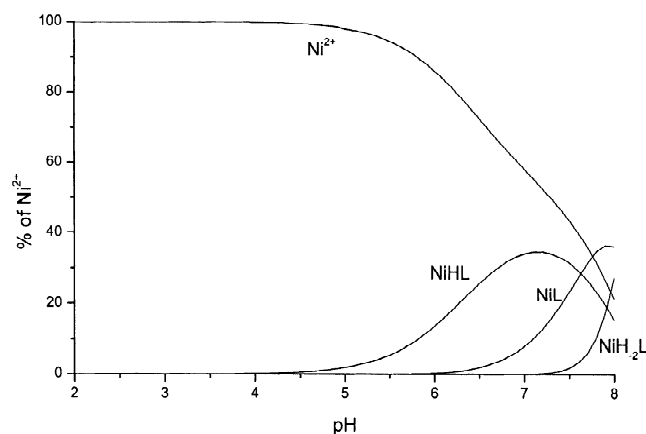


Fig. 2. Species distribution for nickel(II)-**fam** system at 1:3 metal to ligand ratio,  $c_L = 2$  mM.

tion. It should be mentioned here that monodentate coordination in the equimolar Ni(II)-imidazole complex results in  $\log K \sim 3.0$ , similar to that of [NiHL]<sup>3+</sup> species (Table 1) [17].

The tetragonal [CuL]<sup>2+</sup> complex, according to previous studies, contained the binding sites centered at three nitrogens and a thioether sulfur atom [3]. Cu(II) coordinated to the drug molecule via guanidine nitrogen N(3) and then thiazole nitrogen N(9), the thioether S(11) and amidine nitrogen N(16) to form a stable complex. In the case of [NiL]<sup>2+</sup> species, such coordination is less likely, although thiazole and guanidine nitrogens are most likely involved in the metal ion binding. The involvement of S(11) in this complex is less favored and, in fact, no characteristic S→Ni(II) charge transfer band could be observed in electronic absorption UV–Vis spectrum [1]. The stability of the octahedral [NiL]<sup>2+</sup> is almost five orders of magnitude (4.77) lower than that of [CuL]<sup>2+</sup> complex (Table 1). Additionally, water molecules most likely coordinate to Ni(II).

When pH increases above 7.5, the [NiL]<sup>2+</sup> species undergoes a two-proton dissociation process and the [NiH<sub>2</sub>L] complex is formed. A similar pattern is observed for peptide ligands when planar complex is formed with simultaneous release of two or three protons [18,19]. As in the case of [NiL]<sup>2+</sup> complex, thiazole and guanidine

Table 1

Protonation constants and Ni(II) complex formation constants of famotidine (L) at  $I = 0.1$  M KNO<sub>3</sub> and 25 °C

Complex	Log $\beta$	pK
[HL] <sup>+</sup>	11.15(1)	11.15 (amide/amidine nitrogen)
[H <sub>2</sub> L] <sup>2+</sup>	17.87(1)	6.72 (thiazole nitrogen)
[NiHL] <sup>3+</sup>	13.69(2)	2.54 <sup>a</sup>
[NiL] <sup>2+</sup>	6.06(2)	7.63
[NiH <sub>2</sub> L]	-10.06(2)	16.12

<sup>a</sup> Stability constants for the first complex after subscription of the protonation constant of the unbound nitrogen donor(s).

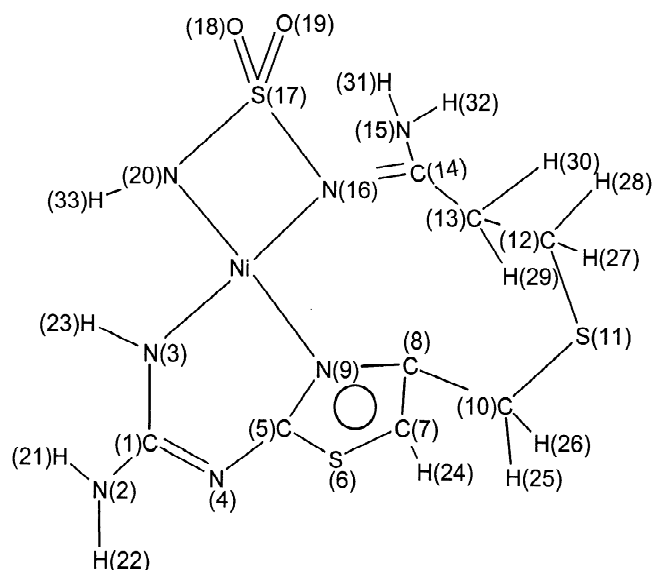


Fig. 3. The proposed structure of nickel(II)-**fam** square-planar complex in the solid state with atom numbering used in calculation.

nitrogens are likely engaged in binding Ni(II) ion to form a planar complex. Additionally, two other nitrogens from the terminal part of the ligand are involved in coordination, i.e. either N(15) or N(16) and N(20).

### 3.2. Geometry of planar Ni(II)-**fam** complex

Based on potentiometric, vibrational and NMR measurements (discussed further) we conduct calculations assuming two structures of square-planar Ni(II)-**fam** complex with coordination of nickel ion by N(3), N(9), N(20) and either N(15) or N(16) nitrogen. Somehow surprisingly, the complex in which N(16) instead of N(15) was involved in Ni(II) binding turned out to be more stable.

The atom numbering used in these calculations is shown in Fig. 3. The lack of imaginary vibrational frequencies after geometry optimization may suggest that the proposed planar structure formed by these four nitrogens with Ni(II) as the central metal ion reaches a global energy minimum.

Table 2

Some calculated bond angles and bond distances of nickel(II)-**fam** square-planar complex in solid state

Numbering of bond angles or distances	Calculated value of bond angles or distances
Ni–N(3)	1.91 Å
Ni–N(9)	1.98 Å
Ni–N(16)	2.20 Å
Ni–N(20)	1.94 Å
N(3)–Ni–N(9)	91.71°
N(3)–Ni–N(20)	95.97°
N(9)–Ni–N(16)	110.93°
N(16)–Ni–N(20)	72.67°
N(3)–Ni–N(16)–N(20)	213.03°
N(9)–Ni–N(20)–N(16)	202.90°

Nitrogen–Ni(II) bond distances and N–Ni(II)–N bond angles for just calculated structure are listed in Table 2. Three Ni–N bonds, where N represents N(3), N(9) and N(20), have a similar length within the 1.91–1.98 Å range. In contrast, the fourth Ni(II)–N bond, i.e. Ni–N(16) is much longer and reaches 2.20 Å causing a slight distortion from the planar structure. However, this elongation of the bond results in stabilization of the four-membered ring formed by N(16), S(17), N(20) atoms and Ni(II) ion, an arrangement that is very rarely encountered. To ease the internal stress of the ring, N(20) moves out of plane formed by the three other atoms. The loss of ring planarity is additionally supported by the values of respective angles, for example, the angle between N(16)–Ni–N(20) atoms is only 72.67° while the three other angles are greater than 90° (Table 2).

### 3.3. Vibrational spectroscopy

FT-IR and Raman spectra of both Ni(II)-**fam** complexes in the solid state are shown in Figs. 4 and 5, respectively. As seen, these spectra have different vibrational patterns confirming that investigated complexes have different molecular structures.

As discussed earlier in the paper, we suggest octahedral coordination for a blue Ni(II)-**fam** complex. A thiazole nitrogen N(9) and one of the two guanidine nitrogens, N(2) or N(3), are the most likely binding sites. Since at this pH proton dissociation from the ligand does not occur, two anions of  $\text{ClO}_4^-$  bind to Ni(II) to compensate for the positive charge of the complex. Moreover, we suggest that two water molecules bind to a Ni(II) ion to fulfil the octahedral coordination sphere that is easily seen by the characteristic colour of the complex. The presence of perchlorate ions is confirmed in FT-IR spectra by the observation of two characteristic features:  $626\text{ cm}^{-1}$  and the broad centered at  $1100\text{ cm}^{-1}$  which are readily assigned to  $\nu_4$  and  $\nu_3$ , respectively, of the anion vibrations (Fig. 4a) [16]. In the Raman spectrum (Fig. 5a) of the octahedral Ni(II) complex, four characteristic  $\text{ClO}_4^-$  vibrations at 456, 626, 925 and  $1100\text{ cm}^{-1}$  can be easily found [16]. The presence of coordinated water molecules in the octahedral Ni(II)-**fam** complex is supported by the observation of two broad bands at  $3435\text{ cm}^{-1}$  (not shown) and  $1673\text{ cm}^{-1}$  in the FT-IR spectrum (Fig. 4a) that are obviously due to O–H stretching and H–O–H bending motions of coordinated  $\text{H}_2\text{O}$ , respectively [16]. Additionally,  $\text{NH}_2$  scissor vibrations can be observed in IR spectra in the  $1600\text{--}1700\text{ cm}^{-1}$  range. Thus, an intense, broad band centered at  $1673\text{ cm}^{-1}$  is due to  $\text{NH}_2$  scissor vibrations from all four amine groups, i.e.  $\text{N}(2)\text{H}_2$ ,  $\text{N}(3)\text{H}_2$ ,  $\text{N}(15)\text{H}_2$  and  $\text{N}(20)\text{H}_2$ , that overlap with H–O–H bending of coordinated water. On the other hand, these vibrations can be found in the Raman spectrum as weak features at  $1675\text{ cm}^{-1}$  (Fig. 5a). However, in this case, the  $1675\text{ cm}^{-1}$  band

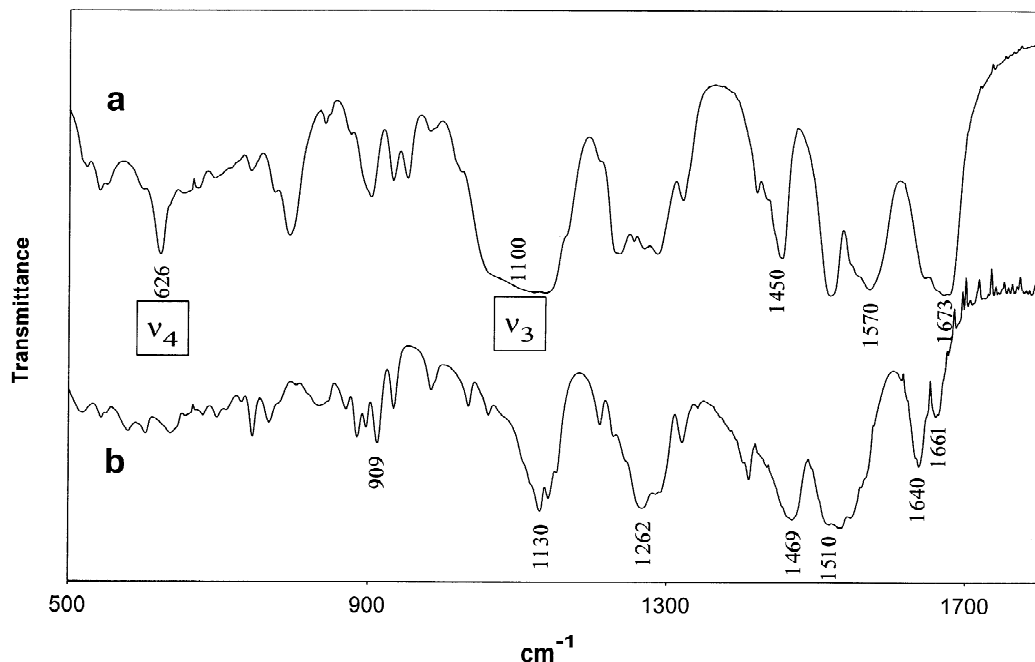


Fig. 4. FT-IR spectra of blue (a) and yellow (b) nickel(II)-fam complexes in the solid state in the 500–3600  $\text{cm}^{-1}$  range.

is mainly due to scissor vibrations of guanidine amine. Other IR strong absorptions in the 1240–1320 and 1500–1580  $\text{cm}^{-1}$  ranges are mainly due to thiazole vibrations; however, in the higher frequency region, the C=N stretching vibrations,  $\nu(\text{C}=\text{N})$ , participate in normal mode composition [20]. The strong 1450  $\text{cm}^{-1}$  band is mainly due to H–C–H bending vibrations of the aliphatic chain. The Raman spectrum (Fig. 5a) supports our assignments, for example, strong thiazole modes at 1318 and 1520  $\text{cm}^{-1}$  are

easily seen in the spectrum. The strong mode at 1551  $\text{cm}^{-1}$  carries a substantial contribution from  $\nu(\text{C}=\text{N})$  of guanidine and thiazole. The thiazole ring ‘breathing’ vibration at 1004  $\text{cm}^{-1}$  (free ligand) is down-shifted to 984  $\text{cm}^{-1}$  in the Raman spectrum upon complex formation. The changes in frequencies presented here can be understood as involvement of guanidine and thiazole nitrogens in Ni(II) ion binding [8,20].

In the case of Ni(II)-**fam** yellowish-orange complex, we

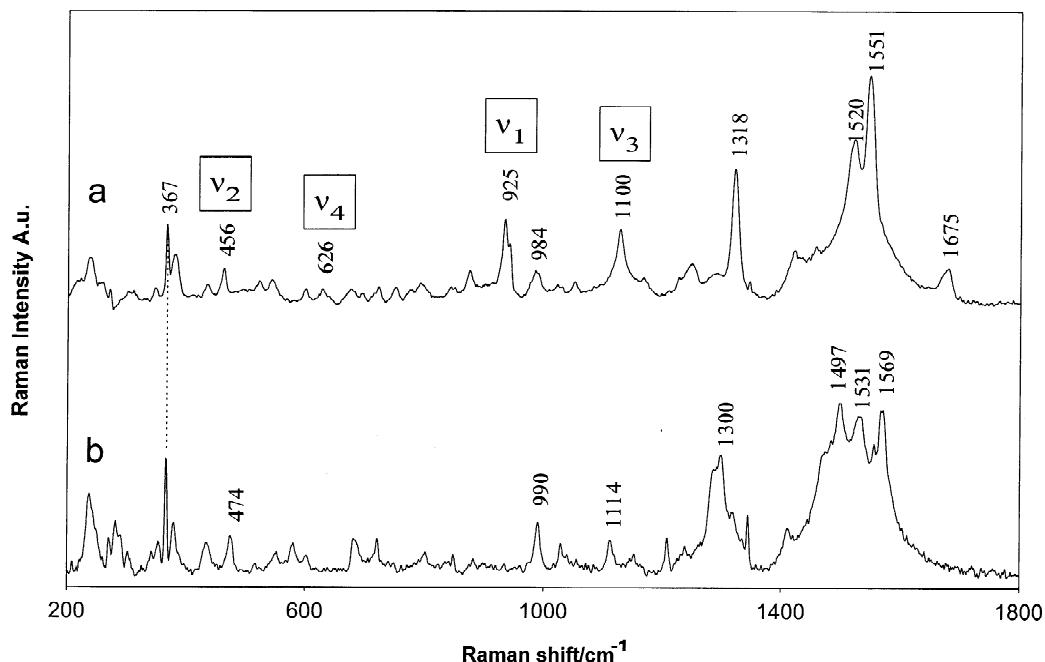


Fig. 5. Raman spectra of blue (a) and yellow (b) nickel(II)-fam complexes in the solid state in the 200–1800  $\text{cm}^{-1}$  range.

assume tetragonal coordination of the metal ion. This is in agreement with potentiometric data (*vide supra*) and characteristic colour for a square-planar nickel(II) complex. As suggested earlier in the paper, **fam** nitrogen donors: N(3), N(9), N(16) and N(20) are involved in Ni(II) binding. Figs. 4b and 5b show FT-IR and Raman spectra, respectively, of this Ni(II)-complex. As seen, there is lack of characteristic anion vibrations in the presented spectra. This confirms that two protons dissociate from the ligand upon complex formation. Additionally, the lack of characteristic IR bands at  $\sim 3450$  and  $1650\text{ cm}^{-1}$  discussed earlier proves that water molecules do not coordinate to a central metal ion in this yellow complex.

Proton dissociations of **fam** during formation of a square-planar Ni(II) complex are also confirmed by changes in the range of N–H stretching vibrations. Upon deprotonation, asymmetric stretchings of N(3)–H<sub>2</sub> and N(20)–H<sub>2</sub> of free ligand disappear and symmetric stretching vibrations of  $\nu(\text{N}(3)\text{--H})$  and  $\nu(\text{N}(20)\text{--H})$  can be seen in the spectrum at  $3273$  and  $3321\text{ cm}^{-1}$ , respectively. Obvious changes are noticed in N–H<sub>2</sub> scissor vibrations. In the FT-IR spectrum (Fig. 4b), they down-shift and split into two observed at  $1640$  and  $1661\text{ cm}^{-1}$ . Also, the  $1675\text{ cm}^{-1}$  Raman band disappears and this can prove that one of the protons dissociates from the guanidine amine group. A very complex Raman envelope in the  $1400\text{--}1580\text{ cm}^{-1}$  range involves not only thiazole vibrations (please note the changes in their frequencies) but also  $\nu(\text{C}=\text{N})$  and possibly NH<sub>2</sub> deformation vibrations. Additionally, down-shifting of thiazole mode from  $1318\text{ cm}^{-1}$  in an octahedral complex compared to  $1300\text{ cm}^{-1}$  in square-planar complex shows slight rearrangement of this ring upon N(9) binding

to Ni(II). This mode also reflects changes in C–C and N–C–N bending modes that pick up some Raman activity when compare to an octahedral complex. A thiazole ring ‘breathing’ mode seen at  $990\text{ cm}^{-1}$  has almost the same frequency as in the blue complex.

The assignment offered above is supported by calculations of vibrational modes of a square-planar Ni(II)-**fam** complex. Since it belongs to C<sub>1</sub> group symmetry thus, all 96 expected vibrations are both IR and Raman active. HF harmonic frequencies are usually larger than experimental values due to neglecting anharmonicity and electron correlation. This may be corrected by applying a scaling factor 0.89. Using visual programs, the calculated modes were assigned to match against experimental data and characteristic group frequencies [14–16]. Experimental and calculated IR spectra of yellow nickel(II)-**fam** complex in the solid state show fairly good agreement and are presented in Fig. 6. Characteristic vibrations in high frequency range are listed in Table 3.

It has to be noticed that vibrational modes below  $1200\text{ cm}^{-1}$  are very complex and full assignment of the modes is very difficult since we are not able, at this time, to determine PED of these modes due to computer time restrictions. The low-frequency region, below  $500\text{ cm}^{-1}$ , is especially interesting and provides information about the structure and bonding of metal–ligand linkage [21]. However, in many cases, like those discussed in the paper, Ni–ligand vibrations are masked by deformation modes of the ligand itself. According to our calculations a strong mixing of  $\nu(\text{Ni}\text{--N})$  and ligand deformation modes appears and complicates the definitive assignment of the bands in the low-frequency region. Despite these difficulties, our

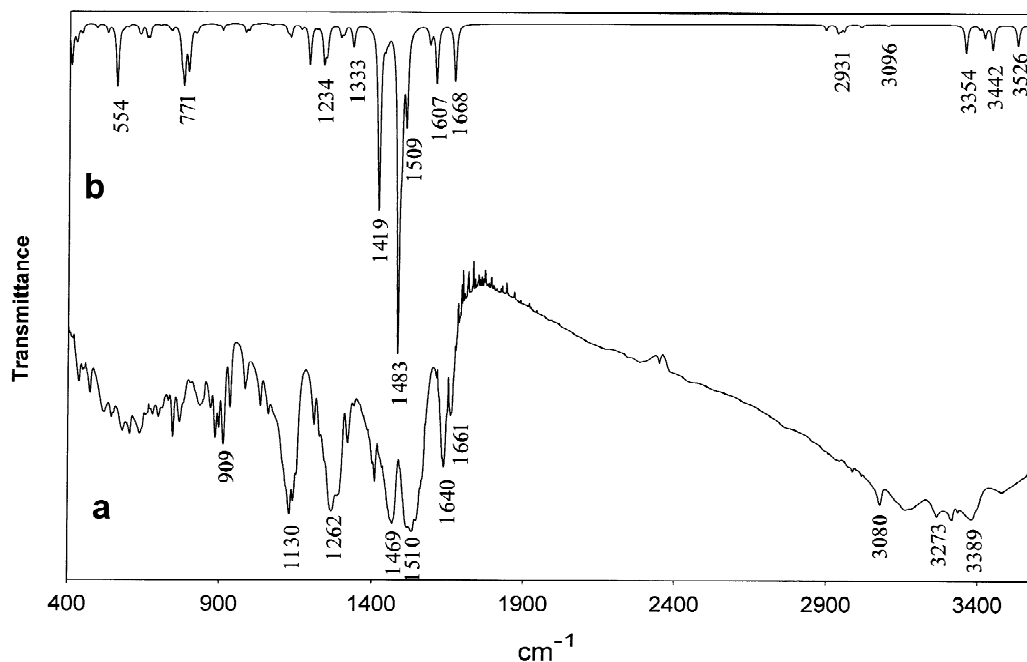


Fig. 6. Experimental (a) and calculated (b) IR spectra of nickel(II)-**fam** square-planar complex in the solid state in the  $400\text{--}3600\text{ cm}^{-1}$  range.

Table 3

Experimental and calculated IR characteristic frequencies of Ni(II)-**fam** square-planar complex and their assignment using ab initio HF/CEP-31G method (scaling factor 0.89) in the range 3600–1200 cm<sup>-1</sup>

IR exp. freq.	Calc. freq.	Assignment
3482	3583	$\nu_{as}(N_2-H)$
3389	3526	$\nu_{as}(N_{15}-H)$
3341	3442	$\nu_s(N_2-H)$
3321	3416	$\nu(N_{20}-H)$
3273	3399	$\nu(N_3-H)$
3188	3354	$\nu_s(N_{15}-H)$
3080	3096	$\nu(C_7-H)$
3018	3008	$\nu_{as}(C_{12}-H)$
3004	3007	$\nu_{as}(C_{10}-H)$
2985	2951	$\nu_{as}(C_{13}-H)$
2961	2940	$\nu_s(C_{10}-H)$
2937	2931	$\nu_s(C_{12}-H)$
2910	2891	$\nu_s(C_{13}-H)$
1661	1668	$\delta(N_{15}-H)$
1640	1607	$\delta(N_2-H)$
1570	1585	$\nu(\text{thiazole})$
1551	1509	$\nu(C_1=N_4), \nu(\text{thiazole})$
1536	1494	$\nu(C_{14}=N_{16})$
1510	1483	$\nu(N_{2,3}-C_1=N_4), \nu(\text{thiazole})$
1469	1448	$\delta(C_{10}-H)$
1445	1447	$\delta(C_{13}-H)$
1428	1438	$\delta(C_{12}-H)$
1410	1419	$\delta(\text{thiazole})$
1400	1413	
1338	1333	$\delta(C-H_2)$
1318	1302	
1293	1292	$\delta(\text{thiazole})$
1262	1249	$\delta(C_{10}-\text{thiazole})$
1243	1246	$\nu(C_1-N_2), \nu(C_1-N_3)$
1223	1234	$\nu(N_3-H), \nu(N_{20}-H)$
1209	1214	$\nu(C-C)$

calculations show that almost all bands in the 200–500 cm<sup>-1</sup> range have a substantial contribution from  $\nu(\text{Ni}-\text{N})$  vibrations. The simulations obtained stopped us from using Ni isotopes to extract the  $\nu(\text{Ni}-\text{N})$  vibrations from vibrational spectra.

### 3.4. <sup>1</sup>H and <sup>13</sup>C and <sup>15</sup>N NMR spectra

Fig. 7 shows <sup>1</sup>H, <sup>13</sup>C and <sup>15</sup>N NMR spectra of a square-planar Ni(II)-**fam** dissolved in DMSO-*d*<sub>6</sub> measured at room temperature. These measurements were possible since the complex is diamagnetic in contrast to the octahedral Ni(II)-**fam**. Chemical shifts are listed in Tables 4–6. Interpretation of spectra was done based on literature data and NMR calculations of famotidine [22,23]. Full integration of <sup>1</sup>H NMR spectrum of the discussed complex (Fig. 7a, Table 4) results in 13 protons supporting the loss of two protons upon complex formation. This deprotonation was also suggested from other methods used in this study.

The complex structure of the quartet observed at 2.45, 2.73, 3.21 and 3.55 ppm is attributed to the H(30), H(29), H(28) and H(27) of two methylene groups, respectively.

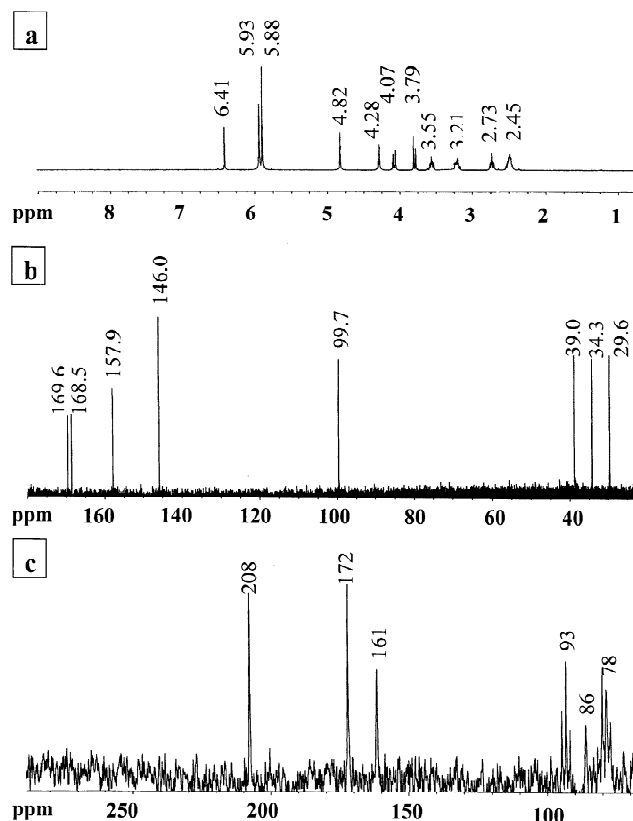


Fig. 7. <sup>1</sup>H NMR (a), <sup>13</sup>C NMR (b), and <sup>15</sup>N NMR (c) spectra of Ni(II)-**fam** square-planar complex in DMSO-*d*<sub>6</sub>.

The observed splitting in these methylene groups in contrast to a free ligand is due to inhibition of a rotation along the C–C bond after complex formation. Two doublets observed at 3.79 and 4.07 ppm are assigned to H(26) and H(25) of methylene hydrogens which are present between the thiazole ring and thioether sulphur S(11) in the aliphatic chain. These protons couple to H(24) thiazole proton despite the fact that they are separated by four bonds. Additional coupling is observed between H(26) and H(25) that confirms inhibition of the rotation of aliphatic chain in the discussed Ni(II) complex. All of the six signals described have integration of 1 thus, each represents a chemical shift of one proton. The signals at 5.88 and 5.93 ppm with integration of 2 each are assigned to two amidine and guanidine hydrogens: H(32,31) and H(22,21), respectively. The methine hydrogen H(24) from the thiazole ring is located at 6.41 ppm. The signals at 4.28 and 4.82 ppm with integration of 1 each belong to two hydrogens: H(33) and H(23), respectively, from a terminal amine group. Their chemical shifts are significantly different from the analogues signals observed in the **fam** spectrum [22]. This suggests the engagement of this part of molecule in coordination of nickel(II) ion.

<sup>13</sup>C NMR (Fig. 7b, Table 5) spectrum of **fam**-Ni(II) shows eight resonance signals from eight carbon atoms and provides additional information about the metal coordina-

Table 4

<sup>1</sup>H NMR chemical shifts  $\delta$  (ppm) of Ni(II)-**fam** square-planar complex in DMSO-*d*<sub>6</sub>

	$\delta$										
	2.45	2.73	3.21	3.55	3.79	4.07	4.28	4.82	5.88	5.93	6.41
Multiplicity	m	m	m	m	d	d	s	s	s	s	s
Integration	1	1	1	1	1	1	1	1	2	2	1
Atom number	H	H	H	H	H	H	H	H	H	H	H
	(30)	(29)	(28)	(27)	(26)	(25)	(33)	(23)	(32,31)	(22,21)	(24)

s, singlet; d, doublet m, multiplet.

Table 5

<sup>13</sup>C NMR chemical shifts  $\delta$  (ppm) of Ni(II)-**fam** square-planar complex in DMSO-*d*<sub>6</sub>

	$\delta$								
	29.6	34.3	39.0	99.7	146.0	157.9	168.5	169.6	
Atom number	C(13)	C(12)	C(10)	C(7)	C(8)	C(1)	C(14)	C(5)	

tion sites in the nickel complex. The sequence of the signals is the same in free and metal bound **fam** [22]. Thus, the chemical shifts at 29.6, 34.3 and 39.0 ppm are attributed to the aliphatic carbons C(13), C(12) and C(10). The next peak observed at 99.7 ppm is assigned to the methine carbon C(7) and is shifted by  $-6.0$  ppm compared to the metal-free ligand [22]. Analogously, other thiazole carbons, i.e. C(5) and C(8) in the nickel complex are shifted by  $-7.9$  and  $-2.9$  ppm (peaks at 169.6 and 146.0 ppm, respectively). These data strongly suggest the engagement of the thiazole ring in binding of nickel ion in the [NiH<sub>2</sub>L] complex. The signals at 157.9 and 168.5 ppm are assigned to C(1) and C(14) carbons. Signal C(14) is shifted by  $+2.4$  ppm upon coordination indicating the involvement of the vicinal nitrogens (N(20), N(16) or N(15)) in metal ion binding combined with an increase in electron density. This can be accounted for by deprotonation in this part of the molecule.

The direct involvement of **fam** nitrogens in the Ni(II) ion binding is clearly indicated by the <sup>15</sup>N NMR spectrum (Fig. 7c, Table 6). The <sup>15</sup>N NMR spectrum of free **fam** consists of three triplets derived from NH<sub>2</sub> groups (both N(2), N(3) and N(15) and N(20)) and three singlets of N(9), N(16) and N(4) nitrogens [22]. The N(2) and N(3) triplets overlap indicating that both nitrogens are magnetically equivalent. Upon metal ion binding, N(9) ( $-57$  ppm), N(16) ( $-38$  ppm) and N(20) ( $-24$  ppm) signals shift considerably (Table 6), as shown in brackets. The

Table 6

<sup>15</sup>N NMR chemical shifts  $\delta$  (ppm) of Ni(II)-**fam** square-planar complex in DMSO-*d*<sub>6</sub>

	$\delta$						
	208	172	161	93	86	78	
Multiplicity	s	s	s	t	s	m	
Atom number	N(9)	N(16)	N(4)	N(15)	N(20)	N(3), N(2)	

s, singlet; t, triplet; m, multiplet.

N(15) signal at 93 ppm remains as a triplet indicating that this NH<sub>2</sub> group is not engaged in the coordination of the Ni(II) metal ion, while N(20) signal at 86 ppm is observed as a doublet indicating loss of one proton. The signal from guanidine nitrogens in Ni(II)-**fam** complex clearly suggests deprotonation and engagement of this part of the molecule in coordination of Ni(II). Thus, <sup>15</sup>N NMR spectra additionally supported by <sup>13</sup>C NMR data show that Ni(II) ion coordinates to **fam** to form a square-planar complex [NiH<sub>2</sub>L], in which the N(9), N(16) and singly deprotonated N(20) and N(3) nitrogens provide binding sites. Thus, such coordination differs markedly from the previously investigated square-planar complex of Cu(II)-**fam** [4].

## Acknowledgements

The authors thank Polfa Pharmaceutical Co. (Starogard Gdański, Poland) for supplying the famotidine sample. We also thank Dr James R. Kincaid (Marquette University, Milwaukee, USA) for permission to use his Raman equipment and Dr Edyta Podstawka for measuring Raman spectra. This work was supported by a grant from the Polish State Committee for Scientific Research (KBN, 3 T09A 125 10 to LMP).

## References

- [1] H. Kozłowski, T. Kowalik-Jankowska, A. Anouar, P. Decock, J. Sychala, J. Świątek-Kozłowska, M.L. Ganadu, J. Inorg. Biochem. 48 (1992) 233.
- [2] C.R. Ganellin, M.E. Parsons, Pharmacology of Histamine Receptors, Wright, Bristol, 1982.
- [3] A.M. Duda, T. Kowalik-Jankowska, H. Kozłowski, T. Kupka, J. Chem. Soc., Dalton Trans. (1995) 2909.
- [4] M. Kubiak, A.M. Duda, M.L. Ganadu, H. Kozłowski, J. Chem. Soc., Dalton Trans. (1996) 1905.

- [5] V. Nurchi, F. Cristiani, G. Crisponi, M.L. Ganadu, G. Lubini, A. Panzanelli, L. Naldini, *Polyhedron* 11 (21) (1992) 2723.
- [6] G. Crisponi, F. Cristiani, V.M. Nurchi, R. Silvagni, M.L. Ganadu, G. Lubini, L. Naldini, A. Panzanelli, *Polyhedron* 14 (11) (1995) 1517.
- [7] M. Barańska, R. Podsiadly, J. Klodowski, L.M. Proniewicz, A. Duda, H. Kozłowski, S. Sanchez-Cortes, J.V. Garcia-Ramos, in: P. Carmona, R. Navarro, A. Hernanz (Eds.), *Spectroscopy of Biological Molecules: Modern Trends*, Kluwer, Dordrecht, 1997, p. 409.
- [8] M. Barańska, Ph.D. Thesis, Jagiellonian University, Cracow, 1998.
- [9] H. Irving, M.G. Miles, L.D. Pettit, *Anal. Chim. Acta* 38 (1967) 475.
- [10] P. Gans, A. Sabatini, A. Vacca, *J. Chem. Soc., Dalton Trans.* (1985) 1195.
- [11] B. Foresman, A. Frisch, *Exploring Chemistry with Electronic Structure Methods*, Gaussian, Pittsburgh, PA, 1993.
- [12] J.A. Pople, H.B. Schlegel, R. Krishnan, D.J. Defrees, J.S. Binkley, M.J. Frisch, R.A. Whiteside, R.F. Hout, W.J. Hehre, *Int. J. Quantum Chem.* S15 (1981) 269.
- [13] J.A. Pople, A.P. Scott, M.W. Wong, L. Radom, *Isr. J. Chem.* 33 (1993) 345.
- [14] D. Lin-Vien, N.B. Colthup, W.G. Fateley, J.G. Grasselli, *The Handbook of Infrared and Raman Characteristic Frequencies of Organic Molecules*, Academic Press, New York, 1991.
- [15] N.P.G. Roeges, *A Guide to the Complete Interpretation of Infrared Spectra of Organic Structures*, Wiley, New York, 1994.
- [16] K. Nakamoto, *Infrared and Raman Spectra of Inorganic and Coordination Compounds*, Wiley, New York, 1997.
- [17] E. Sjöberg, *Pure Appl. Chem.* 69 (1997) 1549.
- [18] L.D. Pettit, J.E. Gregor, H. Kozłowski, in: R.W. Hay, J.R. Dilworth, K.B. Nolan (Eds.), *Perspectives on Bioinorganic Chemistry*, JAI Press, London, 1991, pp. 1–41.
- [19] H. Sigel, R.B. Martin, *Chem. Rev.* 82 (1982) 385.
- [20] J.V. Metzger, in: *Thiazole and its Derivatives*, Vol. 34, Wiley, New York, 1979, Part I.
- [21] M. Barańska, L.M. Proniewicz, *J. Mol. Struct.* 511 (1999) 153.
- [22] M. Barańska, K. Czarniecki, L.M. Proniewicz, *J. Mol. Struct.* (2001) 563.
- [23] C.J. Pouchert, J. Behnke, *The Aldrich Library of <sup>13</sup>C and <sup>1</sup>H FT-NMR Spectra*, 1993.